

UCLA

UCLA Previously Published Works

Title

Sex differences in insular functional connectivity in response to noxious visceral stimulation in rats

Permalink

<https://escholarship.org/uc/item/81f9m3tp>

Authors

Wang, Zhuo
Guo, Yumei
Mayer, Emeran A
et al.

Publication Date

2019-08-01

DOI

10.1016/j.brainres.2019.04.005

Peer reviewed



Published in final edited form as:

Brain Res. 2019 August 15; 1717: 15–26. doi:10.1016/j.brainres.2019.04.005.

Sex differences in insular functional connectivity in response to noxious visceral stimulation in rats

Zhuo Wang^{a,*}, Yumei Guo^a, Emeran A. Mayer^c, Daniel P. Holschneider^{a,b}

^aDepartment of Psychiatry & Behavioral Sciences, University of Southern California, Los Angeles, CA 90089, USA

^bDepartments of Neurology, Biomedical Engineering, University of Southern California, Los Angeles, CA 90089, USA

^cDepartments of Medicine, Physiology, Psychiatry and Biobehavioral Sciences, G Oppenheimer Center for Neurobiology of Stress and Resilience, University of California Los Angeles, Los Angeles, CA 90095, USA

Abstract

Insular cortex (INS) plays a critical role in pain processing and shows sex differences in functional activation during noxious visceral stimulation. Less is known regarding functional interactions within the INS and between this structure and other parts of the brain. Cerebral blood flow mapping was performed using [¹⁴C]-iodoantipyrine perfusion autoradiography in male and female rats during colorectal distension (CRD) or no distension (controls). Forty regions of interest (ROIs) were defined anatomically to represent the granular, dysgranular, and agranular INS along the anterior-posterior (A-P) axis. Inter-ROI correlation matrices were calculated for each group to characterize intra-insular functional connectivity (FC). Results showed a clear FC segregation within the INS into an anterior (rostral to bregma +2.4mm), a posterior (caudal to bregma -1.2 mm), and a mid INS subregion in between. Female controls showed higher FC density compared to males. During CRD, intra-insular FC density decreased greatly in females, but only modestly in males, with a loss of long-range connections between the anterior and mid INS noted in both sexes. New functional organization was characterized in both sexes by a cluster in the mid INS and primarily short-range FC along the A-P axis. Seed correlation analysis during CRD showed sex differences in FC of the anterior and mid agranular INS with the medial prefrontal cortex, thalamus, and brainstem areas (periaqueductal gray, parabrachial nucleus), suggesting sex differences in the modulatory aspect of visceral pain processing. Our findings suggest presence of substantial sex differences in visceral pain processing at the level of the insula.

*Corresponding author at: Department of Psychiatry & the Behavioral Sciences, Keck School of Medicine, University of Southern California, 1333 San Pablo St, MCA-B5, Los Angeles, CA 90033, USA. zhuowang@usc.edu (Z. Wang).

Author contribution

ZW, EAM, and DPH designed research; ZW and YG performed experiments; ZW and DPH analyzed data; ZW, EAM, and DPH wrote the paper.

Declaration of interest

None.

Appendix A. Supplementary data

Supplementary data to this article can be found online at <https://doi.org/10.1016/j.brainres.2019.04.005>.

Keywords

Insular cortex; Functional connectivity; Sex differences; Visceral pain; Colorectal distention

1. Introduction

The insular cortex (INS) is generally considered a center for interoception, where information arising from the viscera is processed and integrated with other sensory, cognitive, and affective information (Craig, 2009). Clinical and basic research has implicated the INS in an astonishingly broad range of functions, including pain, visceral sensation, motor control, cognition, and emotion among others (Nieuwenhuys, 2012). This diversity in INS function suggests heterogeneity in subregional and circuit-level organization (Shura et al., 2014). Recently, meta-analysis of task-related activation in the INS and functional connectivity (FC)-based cluster analysis of human resting-state functional magnetic resonance imaging (rs-fMRI) data have shed new light on the functional differentiation of the INS (Kurth et al., 2010; Cauda et al., 2011; Deen et al., 2011; Cloutman et al., 2012; Chang et al., 2013; Uddin et al., 2014; Fan et al., 2016). While details differ, these neuroimaging studies collectively suggest functional segregation along the anterior-posterior (A-P) axis, and likely a dorsolateral subdivision in the anterior INS. Differential structural and resting-state FC have also been reported for the anterior, mid, and posterior insula with other pain-relevant brain regions in human (Wiech et al., 2014).

Much has been learned about the structure and function of the INS through investigation in rodents. The INS, from its dorsal to ventral aspect, consists of cytoarchitecturally distinct granular (G), dysgranular (D), and agranular (A) zones, with the part of agranular INS rostral to the bregma being further subdivided into a dorsal (Ad) and a ventral component (Av) (Paxinos and Watson, 2005). In support of an integrative function of the INS, tract tracing studies have shown afferent and efferent connections of the INS with broad areas of the brain, including prefrontal, motor, sensory, and association cortical areas, as well as limbic (amygdala, thalamus, subiculum), striatal, and brainstem areas (periaqueductal gray [PAG], dorsal raphe, and parabrachial nucleus) (Shipley, 1982; Guldin and Markowitsch, 1983; Cechetto and Saper, 1987; Krushel and van der Kooy, 1988; Allen et al., 1991; Yasui et al., 1991; Shi and Cassell, 1998b; Jasmin et al., 2004; Zingg et al., 2014). In contrast to this well-established understanding of the INS neuroanatomy, functional segregation and functional connectivity of the INS in association with different behavioral states remain largely unknown. The present study begins to address this knowledge gap in a rat model during exposure to noxious visceral stimulation.

The INS plays a critical role in visceral pain processing and shows sex differences in its functional activation during noxious visceral stimulation in both humans (Berman et al., 2000; Kern et al., 2001; Naliboff et al., 2003; Berman et al., 2006; Kano et al., 2013) and rodents (Wang et al., 2009). Disease and sex-related alterations in insular reactivity and resting-state FC, have been reported in chronic pain conditions, including irritable bowel syndrome (IBS) (Maleki et al., 2012; Ichescio et al., 2014; Hong et al., 2016; Gupta et al., 2017). Sex differences in circuit-level functional interactions, both within the INS and with

other parts of the brain, are just beginning to be investigated (Hong et al., 2014; Dai et al., 2018). To characterize sex differences in insular FC in rats during noxious visceral stimulation, we applied new FC analysis to a published autoradiographic cerebral blood flow (CBF, as a proxy measure for neuronal activity) mapping data set (Wang et al., 2008, 2009) in which sex differences in brain responses to visceral pain were investigated using the colorectal distension model (Ness and Gebhart, 1988). To our best knowledge, insular FC has only been examined in resting-state in human fMRI studies, but not in acute state of pain. And there has not been rodent neuroimaging report on insular FC. We aim to fill these knowledge gaps. Understanding sex- and pain-related changes in insular FC in rodent model is critical for bridging human and animal research, and for guiding future mechanistic research in animals at molecular (neurochemistry) and cellular (tract tracing) level.

2. Results

Autoradiographic CBF mapping was performed in the CRD model of experimental visceral pain in 4 groups of rats: male/control, male/distended, female/control, female/distended.

Regional CBF was quantified by autoradiography and analyzed in 3-dimensionally reconstructed brains. Forty unilateral regions of interest (ROIs) in the INS were defined manually in the left hemisphere of a template brain, to which all brains were spatially normalized. One ROI was drawn for each cytoarchitectural INS zone on one coronal section of the template with a 0.6 mm inter-section interval (Fig. 1). Each ROI label contained an index number denoting its A-P location. Mean optical density of each ROI was extracted for each animal.

2.1. Sex and CRD-related differences in intra-insular functional connectivity

Pearson's correlation coefficients between pairs of ROIs were calculated across subjects within each group to construct intra-INS correlation matrices. Controls showed strong intra-insular FC with females showing higher density (the number of connections as a proportion of the maximum possible number of connections) at 0.34 compared to males at 0.15 (Fig. 2A, B). Clear functional segregation was seen along the A-P axis, with the demarcation of a distinct posterior insular subregion caudal to bregma -1.2 mm (approximate border between index #9 and #10). Females showed significantly more FC anterior to the division, whereas males showed significantly more FC in the posterior INS (Fig. S4A, Fisher's Z transform, $P < 0.05$). During CRD, intra-insular FC density was 0.13 in females (-6.2% compared to controls) and 0.14 in males (-7% compared to controls) (Fig. 2C, D). New functional segregation appeared along the A-P axis between bregma $+2.7$ mm (index #3) and $+2.1$ mm (index #4) (approximate border at bregma $+2.4$ mm). These segregations observed in the control and distended groups divided the INS into an anterior (rostral to bregma $+2.4$ mm), a mid (between bregma $+2.4$ and -1.2 mm), and a posterior subregion (caudal to bregma -1.2 mm). Compared to controls, distension caused statistically significant loss of connection *within* the anterior and mid INS in females (Fig. S4C), but not in males (Fig. S4D). In fact, distension in males resulted in no substantial change in connectivity density *within* any insular subregions, whereas females were unaffected only for the FC *within* the posterior INS. In both sexes, distension resulted in sharp decreases in connectivity density *between*

the anterior and mid INS, but small increases in connections *between* the posterior INS and the other subregions. Next, we calculated the length of functional connections along the A-P axis between any two ROIs as the difference in index number (e.g. the length of D3 ↔ Ad7 is 4; the length of G3 ↔ Av3 is 0.). This revealed that in females, CRD resulted in a 50% decrease in short-range FC (length = 2) and an 84% decrease in long-range FC (length = 3). In males, CRD caused a 21% *increase* in short-range FC and a 78% decrease in long-range FC. The loss of long-range FC was primarily between the anterior and mid INS in both sexes. In the distended groups, there was a persistence of an inter-connected cluster in the mid INS and primarily short-range FC along the A-P axis (significant correlations near the upper-left to lower-right diagonal line in Fig. 2).

Degree analysis identified network hubs, which are marked with symbol 'x' in the schematic INS flat map (Fig. 3). While network hubs were found in both the anterior and mid INS in the control groups, most hubs fell in the mid INS in the distended groups, with a predominance of ventral agranular ROIs in the mid INS emerging as hubs in the female group.

Cytoarchitectural zone-specific FC in the insula was further examined in Fig. 4. This showed the connectivity density in female/control animals to be higher than in male/control animals for all connections within and between insular zones. CRD-induced FC loss was substantial in females, particularly of the granular zone, G-A (−87%), G-D (−82%), D-D (−72%), G-G (−70%), D-A (−55%), and A-A (−29%). CRD-induced FC changes in males were more modest, showing decreases in G-D (−38%), D-D (−36%), and G-A (−29%), no change in G-G, and increases in A-A (+12%) and D-A (+11%). This display clarifies that the CRD-induced FC loss in females was near complete in the anterior INS, with residual connections in the mid and posterior INS noted mostly for dysgranular and agranular ROIs. Fig. 4 also highlights the loss of long-range FC in the distended groups (females, males) compared to controls, with remaining FC predominantly being short-range and between neighboring ROIs.

2.2. Sex and CRD-related differences in whole-brain functional connectivity of the insular cortex

Seed correlation analysis was done for every insular ROI in every group to assess whole-brain level FC. The number of voxels across the whole brain (including the INS) showing statistically significant correlation with the seed was counted as a proportion of the total number of voxels in the template brain, and is summarized in Fig. 5. The female/control group showed the highest level of whole-brain FC at 0.20 (mean of 40 ROIs), which was reduced to 0.14 (−30%) in the female/distended group. In contrast, the average FC level in the male/control and male/distended group was 0.12 and 0.14 (+17%), respectively. ROIs with the highest level of whole-brain FC were noted in the mid INS in the females, and in the anterior and mid INS in the males.

2.3. Sex and CRD-related differences in insular functional connectivity with pain-related brain regions

To evaluate region-specific FC of the INS across the whole brain, correlation matrices were calculated between the 40 insular ROIs and 20 structural ROIs representing brain regions implicated in pain processing with known structural connections with the INS (Fig. 6A, B, D, E). Sex-related differences in FC were further analyzed and presented in Fig. 6C and F.

In the female/control group (Fig. 6A), the anterior and mid INS showed similar FC pattern: positive FC with the infralimbic area of the medial prefrontal cortex and somatosensory cortex (primary and secondary), and lateral hypothalamus. The posterior INS showed positive FC with the amygdala (basomedial, basolateral, central, and lateral nuclei) through agranular ROIs. In the male/control group (Fig. 6B), the anterior and mid INS showed positive FC with the amygdala, thalamus (ventral posteromedial and ventral posterolateral nuclei), nucleus accumbens, and parabrachial nucleus; and negative FC with the parvicellular part of the ventral posterior nucleus of the thalamus. The mid INS was also positively connected with somatosensory cortices. The posterior INS showed positive FC with the cingulate and somatosensory cortices, amygdala (basomedial and central nuclei), and thalamus (ventral posteromedial and ventral posterolateral nuclei); and negative FC with lateral nucleus of the amygdala, mediodorsal nucleus of the thalamus, PAG, and dorsal raphe. Statistically significant sex differences in the control groups were noted with the insula's FC with the cingulate and somatosensory cortices, amygdala (basolateral and lateral nuclei), and brainstem areas (PAG, dorsal raphe, parabrachial nucleus) (Fig. 6C).

In the female/distended group (Fig. 6D), the anterior INS showed positive FC with the lateral orbital (through Ad1, Av1) and secondary somatosensory cortices, and nucleus accumbens; and negative FC with the lateral orbital (through Ad3) and prelimbic cortices, and ventral posteromedial thalamic nucleus. The mid INS showed positive FC with the ventral orbital and secondary somatosensory cortices, central nucleus of the amygdala, ventral posterolateral thalamic nucleus, and nucleus accumbens; and negative FC with the prelimbic cortex, mediodorsal thalamic nucleus, and PAG. The posterior INS showed positive FC with the ventral orbital cortex, ventral posterolateral thalamic nucleus; and negative FC with the parvicellular part of the ventral posterior nucleus of the thalamus. In the male/distended group (Fig. 6E), similar pattern of FC were noted along the A-P axis. Positive FC was noted with the lateral orbital, ventral orbital, prelimbic, infralimbic, and somatosensory cortices, as well as with the amygdala (basolateral and central nuclei), and nucleus accumbens. Broad negative FC was noted with the thalamus and brainstem areas. Compared to the female/distended group (Fig. 6F), statistically significant sex differences were noted primarily in the anterior INS and the rostral part of mid INS in their FC with the medial prefrontal (prelimbic, infralimbic) and lateral orbital cortices, thalamus, and brainstem areas.

Fig. 7 highlights sex and CRD-related differences in insular FC with the prelimbic area of the prefrontal cortex. The strength of prelimbic FC with individual insular ROIs is color coded in insular flat maps (Fig. 7, left column). CRD induced negative FC between the anterior/mid INS and the prelimbic cortex in females, but positive FC in males.

Representative seed correlation results using Ad4 as the seed further showed this striking sex difference (Fig. 7, right column).

Fig. 6 also revealed a strong, positive functional connection between the mid INS and ventral orbital cortex (VO) in the female/distended, but not other groups. Seed correlation analysis using Ad7 as seed showed this highly specific functional interaction, as well as a strong, negative connection with the periaqueductal gray (PAG) (Fig. S5 of the Supplemental Material).

3. Discussion

We took a data-driven approach to investigate sex and visceral pain-related differences in the INS functional connectivity. To our best knowledge, this is the first effort to systematically map both internal and whole-brain FC of the INS in rodents at the mesoscopic level. Our main findings are as follows. (1) Based on functional segregation of intra-insular FC along the A-P axis, the INS could be subdivided into anterior, mid, and posterior subregions. (2) Females compared to males showed greater density in both internal and whole-brain FC, and greater loss of FC during visceral pain. (3) Visceral pain was associated with a loss of long-range intra-insular connections, particularly between the anterior and mid INS, while the remaining networks were characterized by predominantly short-range connections and mid INS hubs. (4) During noxious visceral stimulation, the anterior and mid INS showed in males significant positive FC with prefrontal cortical areas and broad negative FC with the thalamus and brainstem, whereas in females they showed negative FC with prefrontal areas.

3.1. Three-compartment parcellation of the insula based on internal functional connectivity

Based on FC segregation, we proposed to subdivide the INS into 3 subregions along the A-P axis: an anterior (rostral to bregma + 2.4 mm), a posterior (caudal to bregma -1.2 mm), and a mid INS in between. No clear pattern of functional segregation was noted along the dorsal-ventral axis across the groups. The mid INS contained an interconnected core that took a central position in the insular network in all groups. Most network hubs belonged to the mid INS. The posterior INS formed a less densely interconnected cluster which was largely separated from the rest of the network in all groups. The anterior INS was more diverse in FC and did not form consistent clusters across the groups.

Subdivision of the INS along the A-P axis has been an evolving issue. Based on connectional and electrophysiological evidence, the INS has been subdivided by Cechetto and Saper (1987) into an anterior (rostral to bregma + 2 mm) and a posterior part (from bregma + 2 mm to bregma -2 mm). Based on patterns of cortical, thalamic, and amygdaloid structural connections, Shi and Cassell extended the INS posteriorly beyond the caudal end of the claustrum and subdivided the INS into three subregions: an anterior (rostral to bregma + 2 mm), a posterior (from bregma + 2 mm to bregma) and a “parietal insular” part (caudal to bregma) (Shi and Cassell, 1998a,b). The FC-based, tripartite parcellation revealed by our data is in general agreement with the latter anatomic parcellation.

3.2. Sex-related differences in the intra-insular functional connectivity

Compared to the male controls, the female controls showed higher intra-insular FC density. The anterior and mid INS were almost fully connected in the females, whereas the posterior INS was almost fully connected in the males. Sex differences in the FC density in the control condition may reflect sex differences in the underlying structural connectivity or in resting-state network dynamics. In the distended groups, intra-insular FC density was similar between females and males following a sharp drop in FC density in females. The drop in FC density may reflect a shift of attention to the noxious visceral stimulation, while switching off network activity noted in the animals at rest (Wang et al., 2012). Cytoarchitectural zone-specific FC comparison (Fig. 4) showed more FC in the agranular zone, but less FC in the dysgranular and granular zones in the female/distended group compared to the male/distended group. These results suggest that in response to noxious visceral stimulation, female rats compared to males may have greater recruitment of the circuit in the agranular zone associated with emotional processing, and less recruitment of the granular zone, which is concerned with visceral sensory processing (Allen et al., 1991; Shi and Cassell, 1998a,b). It is recently reported that women showed higher interoceptive awareness than men (Grabauskaite et al., 2017). Considering that the INS is an interoceptive center of the brain and despite possible inter-species differences, it may be postulated that higher intra-insular FC in the female compared to male controls reflect higher interoceptive processing and awareness in female rats at rest. Further research is needed to better understand the biological meaning of these sex differences.

3.3. Visceral pain-related differences in the intra-insular functional connectivity

Comparing the distended and control groups showed clear network reorganization due to noxious visceral stimulation: (1) Long-range connections along the A-P axis between the anterior and mid INS were diminished in the distended groups; (2) reorganized networks preserved a mid INS cluster as the network core and featured predominately short-range connections along the A-P axis; and (3) the posterior INS which was largely disconnected from the rest of the INS in the control groups, was integrated into the INS network in the distended groups. Tract tracing studies have documented extensive reciprocal connections within the INS along both the A-P and the dorsolventral axis (Shi and Cassell, 1998a,b). In our study, both male and female distended groups, demonstrated within-zone FC densities that exceeded between-zone FC densities, i.e. functional connections along the A-P axis exceeded those in the dorso-ventral axis. Much evidence exists in support of a posterior-to-anterior flow of information in the human INS with three stages, arrival and processing of interoceptive and other sensory information posteriorly (granular zone), integration with inputs from other neural resources in the middle, and eventual instantiation of emotion and cognition anteriorly (agranular zone) (Craig, 2010). The FC data presented here are consistent with such a cascade of information flow along the A-P axis, although the correlation-based analysis does not provide information about directionality.

3.4. Sex and visceral pain-related differences in the whole-brain functional connectivity of the insula

In the male/distended group, the anterior/mid INS showed positive connections with the medial prefrontal cortex (including the prelimbic and infralimbic cortices), anterior cingulate cortex (ACC or Cg1), lateral and ventral orbital cortices. In contrast, in the female/distended group, the anterior/mid INS showed *negative* connections with the medial prefrontal cortex and ACC, and positive connections with lateral and ventral orbital cortices. The prelimbic area of medial prefrontal cortex in rodents has features of the dorsolateral prefrontal cortex and perigenual ACC in primates (Preuss, 1995; Uylings et al., 2003; Vertes, 2006), while the infralimbic cortex has features of infragenual ACC (Preuss, 1995). The prefrontal cortex and ACC have been implicated in executive control (Dalley et al., 2004), as well as top-down modulation of pain (Calejesan et al., 2000; Lorenz et al., 2003; Bushnell et al., 2013; Gu et al., 2015; Kang et al., 2015; Wang et al., 2015). These data suggest important sex differences in how the INS interacts with pre-frontal cortical regions, which may underlie sex differences in the processing and modulation of pain and other emotions. In humans, there have been only a few studies examining sex differences in the functional interactions between the INS and these prefrontal regions. Based on resting-state FC analysis of fMRI data, Hong et al. (2014) reported that the right dorsal anterior INS is positively connected to the right medial prefrontal cortex in both male healthy controls and male IBS subjects, but negatively connected in both female healthy controls and female IBS subjects. Dai et al. (2018) reported increased resting-state FC in male compared to female healthy subjects between the left dorsal dysgranular INS and right rostral ACC. Although these sex differences were noted in resting-state in humans, the noteworthy parallel with present findings in rats during CRD suggests sex-dependent interaction of the INS with medial prefrontal cortex across species.

Sex and CRD-related differences were also noted in other brain areas implicated in pain processing and modulation, including the somatosensory cortex, amygdala, thalamus, and brainstem. Our data suggest that in the control state, the INS in male rats interacted extensively with relay regions of the ascending afferent input from the viscera (parabrachial nucleus and thalamic nuclei), and regions concerned with emotional processing (amygdala) and descending modulation (PAG). The INS in female rats primarily interacted with somatosensory cortices.

In the distended groups, the INS demonstrated positive FC to the central amygdaloid nucleus in both males and females, and to the basolateral amygdaloid nucleus in males. While males and females had similar pattern in INS-thalamic, INS-brainstem FC, they differed in extent. Males compared to females showed strikingly broader negative FC between all INS subregions and the thalamus and brainstem. The INS in females showed negative FC with limited areas of the thalamus (mediodorsal, ventral posteromedial nuclei, parvocellular part of the ventral posterior thalamic nuclei) and brainstem (PAG, trend in parabrachial gray); and positive FC with the ventral posterolateral thalamic nucleus. The deactivation and negative cortical FC of thalamic nuclei and parabrachial nucleus may reflect cortical inhibition of these relay centers for visceral input (Wang et al., 2008). The PAG is in general implicated in descending pain inhibition, although it can also mediate pain facilitation

(Vanegas and Schaible, 2004). Deactivation and negative cortical FC of the PAG may reflect inactivation of the PAG-mediated descending pain modulation in this model of visceral pain.

3.5. Translational and other considerations

While general similarities in cytoarchitecture, structural connection, and function of the INS exist across species, it is important to note that there are also major differences (Craig, 2009; Butti and Hof, 2010; Nieuwenhuys, 2012). In primates, the INS consists of an anterior agranular region, a posterior granular region, and a dysgranular region in between (Mesulam and Mufson, 1982; Augustine, 1996). In rodents, the INS has a different orientation, with a ventral agranular, a dorsal granular, and a dysgranular zone in between, while all zones extend along the A-P axis (Cechetto and Saper, 1987; Shi and Cassell, 1998b). Important differences between primates and rodents also exist in the organization of ascending pathways from the spinal cord to the INS (Craig, 2002). The INS in humans and some other mammals contains large, spindle-shaped von Economo neurons, which are not found in rodents (Butti and Hof, 2010). Certain functions involving the INS in humans may be substantially different or not applicable in rodents, such as self-awareness and language. Therefore, caution needs to be taken when comparing human and rodent neuroimaging findings concerning the INS.

We acknowledge some limitations of our study. Autoradiographic measures of brain FC were obtained at a single time point. This approach differs from the intra-subject cross correlation analysis often used on fMRI time series data (Pawela et al., 2008; Magnuson et al., 2010; Liang et al., 2011). Caution needs to be taken comparing FC results between different brain imaging modalities (fMRI, PET, EEG) and between different analytic methods (Di and Biswal, 2012; Buckner et al., 2013; Hutchison et al., 2013; Scholvinck et al., 2013; Wehrli et al., 2013). Different analytic tools have been adapted to allow the determination of functional associations, either by examining the temporal aspects of time series within subjects or, as in the current study, by modeling the system over an experimental period across subjects (Stephan, 2004). While many regions exhibit congruent effects under both analytic approaches (Honey et al., 2007), in some regions the two analyses produce divergent results (Roberts et al., 2016). The advantages and limitations of each analytic method, their applicability to studies of task activation or resting state, and their interpretation with regards to neural activity, brain metabolism and cerebral structure are issues of ongoing investigation (Handwerker et al., 2004; Buckner et al., 2013; Hutchison et al., 2013). Compared to other rodent functional neuroimaging methods, the autoradiographic perfusion method of brain mapping has a favorable combination of features, including the ability to map brain activity in awake, unrestrained animals (which is particularly important for pain and other behavioral research in animals), high spatial resolution (~ 0.1 mm), and good temporal resolution (~ 10 s).

We also acknowledge that insular FC was evaluated in only one type of pain state (CRD-induced visceral pain). It would be important to examine insular FC during other types of experiment pain, as well as in chronic pain models. To what extent changes in insular FC mediate pain processing remain to be evaluated using known analgesics. It may be postulated that certain aspect of insular FC reported here is independent of pain modality

(considering the extensive neuroimaging evidence showing INS responses to different pain modalities) and that there is modality-specific recruitment of the insular circuit during pain processing.

3.6. Conclusions

Our functional connectivity analysis revealed important sex differences in internal and whole-brain functional connectivity of the insular cortex at rest and during noxious visceral stimulation, which may underlie sex differences in the affective/motivational and modulatory aspect of visceral nociceptive processing. The results highlight an urgent need for investigation of possible sex differences in structural connectivity of the insular cortex, as well as for a better understanding of sex differences in the excitatory/inhibitory circuits within the insula and across the pain circuit (e.g., Fernandez et al. (2015)). The mesoscopic level functional connectivity analysis presented here offers a unique map that may be useful for such investigation.

4. Experimental procedure

4.1. Functional brain mapping data

Data collection has been described in details previously (Wang et al., 2009). Adult, male and female Wistar rats (3 months old, Harlan Inc., Indianapolis, IN, USA) were randomized into four groups: male/control ($n = 12$), male/distended ($n = 12$), female/control ($n = 10$), female/distended ($n = 12$). The rats were individually housed on a 12 h light/12 h dark cycle with free access to water and rodent chow. The experiments were conducted under a protocol approved by the Institutional Animal Care and Use Committee of the University of Southern California and in accordance with ethical guidelines for investigations of experimental pain in conscious animals provided by the International Association for the Study of Pain. For radiotracer injection, the animals were cannulated through the right external jugular vein 1 week before the CBF mapping experiments. To measure abdominal electromyographic responses to CRD, electrodes were implanted in the left external oblique musculature and connected to an infrascapular, subcutaneous telemetry transmitter (TA10ETA-F20, Data Sciences Intl., St. Paul, MN, USA). The animals were allowed to recover for 7 days and were habituated to an inserted, uninflated colorectal balloon and an experiment cage for 45 min per day for 3 days prior to CBF mapping. Under a 3 min isoflurane sedation, a latex balloon (length = 6 cm) was inserted intra-anally such that its caudal end was 1 cm proximal to the anus. A silicone tubing connecting the balloon and a barostat (Distender Series II, G&J Electronics, Toronto, Canada) was fixed to the base of the tail with adhesive tape and covered by a protective stainless steel spring. The animals were allowed to recover for 30 min in the experiment cage. At the end of the recovery period, a piece of tubing filled with a radiotracer, [^{14}C]-iodoantipyrine (125 $\mu\text{Ci}/\text{kg}$ in 300 μL of 0.9% saline, ARC, St. Louis, MO, USA) was connected to the animal's cannula on one end, and to a syringe filled with euthanasia agent (pentobarbital 75 mg/kg, 3 mol/L potassium chloride) on the other. The unrestrained animal was allowed to rest for 5 min before receiving a distension of 60-mmHg (distended group) or 0-mmHg (control group) with 60 s duration. Thirty-five seconds after the onset of distension, the radiotracer was infused by a motorized pump at 2.25mL/min, followed immediately by euthanasia, which resulted in

cardiac arrest within ~ 10 s, termination of brain perfusion, and death. This 10 s time window provided the temporal resolution during which the distribution of regional CBF-related tissue radioactivity was mapped. Brains were rapidly removed, flash frozen in methylbutane on dry ice, and later cryosectioned into 20- μ m thick coronal slices (interslice spacing 300 μ m). The slices were exposed for 2 weeks to Ektascan Diagnostic Film (Eastman Kodak, Rochester, NY, USA), and autoradiographic images were digitized on an 8-bit gray scale.

4.2. Image preprocessing

Regional CBF was quantified by autoradiography and analyzed on a whole-brain basis using statistical parametric mapping (SPM, version SPM5, Wellcome Centre for Neuroimaging, University College London, London, UK) (Friston et al., 1990, 1991). For each animal, a 3-dimensional brain was reconstructed using 57 serial coronal sections (voxel size: 40 \times 40 \times 300 μ m). Adjacent sections were aligned both manually and using TurboReg, an automated pixel-based registration algorithm implemented in ImageJ (version 1.35) (Schneider et al., 2012). One “artifact free” brain was selected as reference. All brains were spatially normalized to the reference brain. Following spatial normalization, the normalized images were averaged to create a final brain template. Each original brain was then spatially normalized into the standard space defined by the template and smoothed with a Gaussian kernel (FWHM = 3 \times voxel dimension). Sex differences in visceromotor responses and regional brain activation have been reported previously (Wang et al., 2008, 2009). The present work is focused on FC analysis.

4.3. Region of interest definition and data extraction

The FC analytic methods have been described previously (Wang et al., 2011, 2012; Holschneider et al., 2014). Forty unilateral regions of interest (ROIs) in the INS were defined manually in MRIcro (version 1.40, <http://www.mccauslandcenter.sc.edu/crn1/tools>) (Rorden and Brett, 2000) in the left hemisphere of the template brain according to a rat brain atlas (Paxinos and Watson, 2005) using the rhinal fissure and external capsule as primary local landmarks. One ROI was drawn for each cytoarchitectural INS zone on one coronal section of the template brain, with an inter-section interval of approximately 0.6 mm. All cytoarchitectural zones were represented along the A-P axis, from bregma + 3.9 mm to bregma -2.7 mm (Fig. 1). Each ROI label contained an index number denoting its A-P location. Mean optical density of each ROI was extracted for each animal using the Marsbar toolbox for SPM (version 0.42, <http://marsbar.sourceforge.net/>) (Brett et al., 2002). Analysis was also performed using unilateral ROIs from the right hemisphere. While FC patterns were qualitatively similar across hemisphere, we noted greater sex and CRD-related differences in the left hemisphere compared to the right hemisphere (see Supplementary Materials Figs. S1–S3). We have therefore focused our reporting on findings from left ROIs for simplicity purposes.

4.4. Intra-insular functional connectivity analysis

We applied inter-ROI correlation analysis to investigate FC. This is a well-established method, which has been applied to analyze rodent brain mapping data of other modalities, including autoradiographic deoxyglucose uptake (Soncrant et al., 1986; Barrett et al., 2003),

cytochrome oxydase histochemistry (Fidalgo et al., 2011; Padilla et al., 2011), activity regulated genes (*c-fos*) (Wheeler et al., 2013), and fMRI (Schwarz et al., 2007; Roberts et al., 2016). In these studies, correlations are calculated in an inter-subject manner, i.e., across subjects within a group. Perfusion mapping using autoradiographic methods presents a ‘snap-shot’ of brain activity at a single point in time, and thus, precludes analysis of the dynamics of functional brain activation (see discussion below). Pearson’s correlation coefficient between each pair of insular ROIs was calculated across subjects within each group in Matlab (version 6.5.1, Mathworks, Inc., Natick, MA, USA) to construct correlation matrices. The ROIs were arranged from anterior to posterior, and from dorsal to ventral at each bregma level. Pearson’s coefficients were transformed into Z values using Fisher’s transformation for statistical analysis. Correlation matrices were visualized as heatmaps in Matlab. To control Type I error attributable to the large number of correlations computed, we implemented a jackknife procedure following Barrett et al. (2003). For a group of n subjects, n iterations were performed in which one subject was dropped sequentially and the correlation matrix was recalculated with the remaining ($n - 1$) subjects. A correlation was considered statistically significant only if $P < 0.05$ in all iterations. These correlation matrices formed the basis for the following degree centrality analysis and cytoarchitectural zone-specific FC analysis.

4.5. Degree centrality

In an intra-insular network, hubs are defined as ROIs that are central to the organization of the network. To identify hubs, we calculated degree centrality, which is defined as the number of statistically significant functional connections. Nodes with degrees ranked in the top 20% are interpreted as hubs.

4.6. Cytoarchitectural zone-specific functional connectivity analysis

To characterize zone-specific FC in the insular network, we plotted within-zone (A-A, agranular; D-D, dysgranular; G-G, granular) and between-zone (D-A, G-D, and G-A) FC separately, and calculated zone specific FC densities.

4.7. Whole-brain level seed functional connectivity analysis

We applied seed correlation analysis in SPM to assess sex and CRD-related differences in whole-brain FC of individual insular ROIs. Threshold for significance was set at $P < 0.05$ at the voxel level and an extent threshold of 100 contiguous voxels.

4.8. Functional connectivity of the insular ROIs with pain-related regions

We have previously proposed to use structural connectivity information to constrain FC analysis, thereby putting more emphasis on direct neural interactions (Wang et al., 2013). To evaluate region-specific FC of the INS, correlation matrices were calculated between the 40 insular ROIs and 20 structural ROIs representing regions implicated in pain processing with known structural connections with the INS (Shipley, 1982; Guldin and Markowitsch, 1983; Cechetto and Saper, 1987; Krushel and van der Kooy, 1988; Allen et al., 1991; Yasui et al., 1991; Shi and Cassell, 1998b; Jasmin et al., 2004). These structural ROIs were drawn in MRICro in the left hemisphere of the template brain. Statistical significance of between-

group difference in correlation coefficients was evaluated using Fisher's Z-transform ($P < 0.05$). It is important to note though that while the insular ROIs were at a mesoscopic level, some ROIs for the other broader brain regions (e.g. primary somatosensory cortex) were at a macroscopic level. Examining FC at a mesoscopic level for all regions would greatly increase the size of the correlation matrix and is beyond the scope of the present study. Therefore, the results should be interpreted as information on the *general* pattern of whole-brain FC of the INS.

Supplementary Material

Refer to Web version on PubMed Central for supplementary material.

Acknowledgements

The research was supported by the United States National Institutes of Health grant P50DK064539 (EAM) and the University of Southern California Zumberge Individual Research Award (ZW). We thank anonymous reviewers at Brain Research for their time and constructive comments.

Abbreviations:

| | |
|-------------|---------------------------------------|
| ACC | anterior cingulate cortex |
| Ad | dorsal agranular insula |
| A-P | anterior-posterior |
| Av | ventral agranular insula |
| CBF | cerebral blood flow |
| CRD | colorectal distension |
| FC | functional connectivity |
| fMRI | functional magnetic resonance imaging |
| IBS | irritable bowel syndrome |
| INS | insular cortex |
| ROI | region of interest |
| SPM | statistical parametric mapping |

References

- Allen GV, Saper CB, Hurley KM, Cechetto DF, 1991 Organization of visceral and limbic connections in the insular cortex of the rat. *J. Comp. Neurol* 311,1–16. [PubMed: 1719041]
- Augustine JR, 1996 Circuitry and functional aspects of the insular lobe in primates including humans. *Brain Res. Brain Res. Rev* 22,229–244. [PubMed: 8957561]
- Barrett D, Shumake J, Jones D, Gonzalez-Lima F, 2003 Metabolic mapping of mouse brain activity after extinction of a conditioned emotional response. *J. Neurosci* 23,5740–5749. [PubMed: 12843278]

- Berman S, Munakata J, Naliboff BD, Chang L, Mandelkern M, Silverman D, Kovalik E, Mayer EA, 2000 Gender differences in regional brain response to visceral pressure in IBS patients. *Eur. J. Pain* 4,157–172. [PubMed: 10957697]
- Berman SM, Naliboff BD, Suyenobu B, Labus JS, Stains J, Bueller JA, Ruby K, Mayer EA, 2006 Sex differences in regional brain response to aversive pelvic visceral stimuli. *Am. J. Physiol. Regul. Integr. Comp. Physiol* 291, R268–R 276. [PubMed: 16614061]
- Brett M, Anton J-L, Valabregue R, Poline J-B, 2002 Region of interest analysis using an SPM toolbox The 8th International Conference on Functional Mapping of the Human Brain. Sendai, Japan.
- Buckner RL, Krienen FM, Yeo BT, 2013 Opportunities and limitations of intrinsic functional connectivity MRI. *Nat. Neurosci* 16,832–837. [PubMed: 23799476]
- Bushnell MC, Ceko M, Low LA, 2013 Cognitive and emotional control of pain and its disruption in chronic pain. *Nat. Rev. Neurosci* 14,502–511. [PubMed: 23719569]
- Butti C, Hof PR, 2010 The insular cortex: a comparative perspective. *Brain Struct. Funct* 214,477–493. [PubMed: 20512368]
- Calejesan AA, Kim SJ, Zhuo M, 2000 Descending facilitatory modulation of a behavioral nociceptive response by stimulation in the adult rat anterior cingulate cortex. *Eur. J. Pain* 4,8–96.
- Cauda F, D'Agata F, Sacco K, Duca S, Geminiani G, Vercelli A, 2011 Functional connectivity of the insula in the resting brain. *Neuroim age* 55,8–23.
- Cechetto DF, Saper CB, 1987 Evidence for a viscerotopic sensory representation in the cortex and thalamus in the rat. *J. Comp. Neurol* 262,27–45. [PubMed: 2442207]
- Chang LJ, Yarkoni T, Khaw MW, Sanfey AG, 2013 Decoding the role of the insula in human cognition: functional parcellation and large-scale reverse inference. *Cereb. Cortex* 23,739–749. [PubMed: 22437053]
- Cloutman LL, Binney RJ, Drakesmith M, Parker GJ, Lambon Ralph MA, 2012 The variation of function across the human insula mirrors its patterns of structural connectivity: evidence from in vivo probabilistic tractography. *Neuroim age* 59,3514–3521.
- Craig AD, 2002 How do you feel? Interoception: the sense of the physiological condition of the body. *Nat. Rev. Neurosci* 3,655–666. [PubMed: 12154366]
- Craig AD, 2009 How do you feel-now? The anterior insula and human awareness. *Nat. Rev. Neurosci* 10,59–70. [PubMed: 19096369]
- Craig AD, 2010 The sentient self. *Brain Struct. Funct* 214,563–577. [PubMed: 20512381]
- Dai YJ, Zhang X, Yang Y, Nan HY, Yu Y, Sun Q, Yan LF, Hu B, Zhang J, Qiu ZY, Gao Y, Cui GB, Chen BL, Wang W, 2018 Gender differences in functional connectivities between insular subdivisions and selective pain-related brain structures. *J. Headache Pain* 19, 24. [PubMed: 29541875]
- Dalley JW, Cardinal RN, Robbins TW, 2004 Prefrontal executive and cognitive functions in rodents: neural and neurochemical substrates. *Neurosci. Biobehav. Rev* 28,771–784. [PubMed: 15555683]
- Deen B, Pitskel NB, Pelphrey KA, 2011 Three systems of insular functional connectivity identified with cluster analysis. *Cereb. Cortex* 21,1498–1506. [PubMed: 21097516]
- Di X, Biswal BB, 2012 Metabolic brain covariant networks as revealed by FDG-PET with reference to resting-state fMRI networks. *Brain Connect.* 2,275–283. [PubMed: 23025619]
- Fan L, Li H, Zhuo J, Zhang Y, Wang J, Chen L, Yang Z, Chu C, Xie S, Laird AR, Fox PT, Eickhoff SB, Yu C, Jiang T, 2016 The Human brainnetome atlas: a new brain atlas based on connective architecture. *Cereb. Cortex* 26, 3508–3526. [PubMed: 27230218]
- Fernandez, Marron de Velasco, E., Hearing M, Xia Z, Victoria NC, Lujan R, Wickman K, 2015 Sex differences in GABA(B)R-GIRK signaling in layer 5/6 pyramidal neurons of the mouse prefrontal cortex. *Neuropharmacology* 95,353–360.
- Fidalgo C, Conejo NM, Gonzalez-Pardo H, Arias JL, 2011 Cortico-limbic-striatal contribution after response and reversal learning: a metabolic mapping study. *Brain Res* 1368, 143–150. [PubMed: 21036158]
- Friston KJ, Frith CD, Liddle PF, Dolan RJ, Lammertsma AA, Frackowiak RS, 1990 The relationship between global and local changes in PET scans. *J. Cereb. Blood Flow Metab* 10, 458–466.

- Friston KJ, Frith CD, Liddle PF, Frackowiak RS, 1991 Comparing functional (PET) images: the assessment of significant change. *J. Cereb. Blood Flow Metab* 11,690–699. [PubMed: 2050758]
- Grabauskaite A, Baranauskas M, Griskova-Bulanova I, 2017 Interoception and gender: what aspects should we pay attention to? *Conscious. Cogn.* 48, 129–137.
- Gu L, Uhelski ML, Anand S, Romero-Ortega M, Kim YT, Fuchs PN, Mohanty SK, 2015 Pain inhibition by optogenetic activation of specific anterior cingulate cortical neurons. *PLoS ONE* 10, e0117746. [PubMed: 25714399]
- Guldin WO, Markowitsch HJ, 1983 Cortical and thalamic afferent connections of the insular and adjacent cortex of the rat. *J. Comp. Neurol* 215, 135–153. [PubMed: 6853769]
- Gupta A, Mayer EA, Fling C, Labus JS, Naliboff BD, Hong JY, Kilpatrick LA, 2017 Sex-based differences in brain alterations across chronic pain conditions. *J. Neurosci. Res* 95,604–616. [PubMed: 27870423]
- Handwerker DA, Ollinger JM, D'Esposito M, 2004 Variation of BOLD hemodynamic responses across subjects and brain regions and their effects on statistical analyses. *Neuroimage* 21, 1639–1651.
- Holschneider DP, Wang Z, Pang RD, 2014 Functional connectivity-based parcellation and connectome of cortical midline structures in the mouse: a perfusion autoradiography study. *Front. Neuroinform* 8,61. [PubMed: 24966831]
- Honey CJ, Kotter R, Breakspear M, Sporns O, 2007 Network structure of cerebral cortex shapes functional connectivity on multiple time scales. *Proc. Natl. Acad. Sci. U.S.A* 104, 10240–10245. [PubMed: 17548818]
- Hong JY, Kilpatrick LA, Labus JS, Gupta A, Katibian D, Ashmead C, Stains J, Heendeniya N, Smith SR, Tillisch K, Naliboff B, Mayer EA, 2014 Sex and disease-related alterations of anterior insula functional connectivity in chronic abdominal pain. *J. Neurosci* 34, 14252–14259. [PubMed: 25339739]
- Hong JY, Naliboff B, Labus JS, Gupta A, Kilpatrick LA, Ashmead C, Stains J, Heendeniya N, Smith SR, Tillisch K, Mayer EA, 2016 Altered brain responses in subjects with irritable bowel syndrome during cued and uncued pain expectation. *Neurogastroenterol. Motil* 28, 127–138. [PubMed: 26526698]
- Hutchinson RM, Womelsdorf T, Allen EA, Bandettini PA, Calhoun VD, Corbetta M, Della Penna S, Duyn JH, Glover GH, Gonzalez-Castillo J, Handwerker DA, Keilholz S, Kiviniemi V, Leopold DA, de Pasquale F, Sporns O, Walter M, Chang C, 2013 Dynamic functional connectivity: promise, issues, and interpretations. *Neuroimage* 80,360–378.
- Ichesco E, Schmidt-Wilcke T, Bhavsar R, Clauw DJ, Peltier SJ, Kim J, Napadow V, Hampson JP, Kairys AE, Williams DA, Harris RE, 2014 Altered resting state connectivity of the insular cortex in individuals with fibromyalgia. *J. Pain* 15 (815–826), e811.
- Jasmin L, Burkey AR, Granato A, Ohara PT, 2004 Rostral agranular insular cortex and pain areas of the central nervous system: a tract-tracing study in the rat. *J. Comp. Neurol* 468, 425–440.
- Kang SJ, Kwak C, Lee J, Sim SE, Shim J, Choi T, Collingridge GL, Zhuo M, Kaang BK, 2015 Bidirectional modulation of hyperalgesia via the specific control of excitatory and inhibitory neuronal activity in the ACC. *Mol. Brain* 8, 81. [PubMed: 26631249]
- Kano M, Farmer AD, Aziz Q, Giampietro VP, Brammer MJ, Williams SC, Fukudo S, Coen SJ, 2013 Sex differences in brain response to anticipated and experienced visceral pain in healthy subjects. *Am. J. Physiol. Gastrointest. Liver Physiol* 304, G687–G699. [PubMed: 23392235]
- Kern MK, Jaradeh S, Arndorfer RC, Jesmanowicz A, Hyde J, Shaker R, 2001 Gender differences in cortical representation of rectal distension in healthy humans. *Am. J. Physiol. Gastrointest. Liver Physiol.* 281, G1512–G1523.
- Krushel LA, van der Kooy D, 1988 Visceral cortex: integration of the mucosal senses with limbic information in the rat agranular insular cortex. *J. Comp. Neurol* 270 39–54,62–133. [PubMed: 2453537]
- Kurth F, Zilles K, Fox PT, Laird AR, Eickhoff SB, 2010 A link between the systems: functional differentiation and integration within the human insula revealed by meta-analysis. *Brain Struct. Funct* 214,519–534. [PubMed: 20512376]

- Liang Z, King J, Zhang N, 2011 Uncovering intrinsic connective architecture of functional networks in awake rat brain. *J. Neurosci* 31, 3776–3783. [PubMed: 21389232]
- Lorenz J, Minoshima S, Casey KL, 2003 Keeping pain out of mind: the role of the dorsolateral prefrontal cortex in pain modulation. *Brain* 126, 1079–1091. [PubMed: 12690048]
- Magnuson M, Majeed W, Keilholz SD, 2010 Functional connectivity in blood oxygenation level-dependent and cerebral blood volume-weighted resting state functional magnetic resonance imaging in the rat brain. *J. Magn. Reson. Imaging* 32,584–592. [PubMed: 20815055]
- Maleki N, Linnman C, Brawn J, Burstein R, Becerra L, Borsook D, 2012 Her versus his migraine: multiple sex differences in brain function and structure. *Brain* 135, 2546–2559. [PubMed: 22843414]
- Mesulam MM, Mufson EJ, 1982 Insula of the old world monkey. I. Architectonics in the insulo-orbitofrontal component of the paralimbic brain. *J. Comp. Neurol* 212,1–22. [PubMed: 7174905]
- Naliboff BD, Berman S, Chang L, Derbyshire SW, Suyenobu B, Vogt BA, Mandelkern M, Mayer EA, 2003 Sex-related differences in IBS patients: central processing of visceral stimuli. *Gastroenterology* 124, 1738–1747.
- Ness TJ, Gebhart GF, 1988 Colorectal distension as a noxious visceral stimulus: physiologic and pharmacologic characterization of pseudoreflexes in the rat. *Brain Res.* 450, 153–169. [PubMed: 3401708]
- Nieuwenhuys R, 2012 The insular cortex: a review. *Prog. Brain Res.* 195, 123–163. [PubMed: 22230626]
- Padilla E, Shumake J, Barrett DW, Sheridan EC, Gonzalez-Lima F, 2011 Mesolimbic effects of the antidepressant fluoxetine in Holtzman rats, a genetic strain with increased vulnerability to stress. *Brain Res* 1387,71–84. [PubMed: 21376019]
- Pawela CP, Biswal BB, Cho YR, Kao DS, Li R, Jones SR, Schulte ML, Matloub HS, Hudetz AG, Hyde JS, 2008 Resting-state functional connectivity of the rat brain. *Magn. Reson. Med* 59, 1021–1029. [PubMed: 18429028]
- Paxinos G, Watson C, 2005 *The rat brain in Stereotaxic Coordinates*, 5th ed Elsevier Academic Press, New York.
- Preuss TM, 1995 Do rats have prefrontal cortex? The rose-woolsey-akert program reconsidered. *J. Cogn. Neurosci* 7, 1–24. [PubMed: 23961750]
- Roberts RP, Hach S, Tippett LJ, Addis DR, 2016 The Simpson's paradox and fMRI: similarities and differences between functional connectivity measures derived from within-subject and across-subject correlations. *Neuroimage* 135,1–15.
- Rorden C, Brett M, 2000 Stereotaxic display of brain lesions. *Behav. Neurol* 12, 191–200. [PubMed: 11568431]
- Schneider CA, Rasband WS, Eliceiri KW, 2012 NIH Image to ImageJ: 25 years of image analysis. *Nat. Methods* 9, 671–675.
- Scholvinck ML, Leopold DA, Brookes MJ, Khader PH, 2013 The contribution of electrophysiology to functional connectivity mapping. *Neuroimage* 80, 297–306.
- Schwarz AJ, Gozzi A, Reese T, Bifone A, 2007 In vivo mapping of functional connectivity in neurotransmitter systems using pharmacological MRI. *Neuroimage* 34, 1627–1636.
- Shi CJ, Cassell MD, 1998b Cortical, thalamic, and amygdaloid connections of the anterior and posterior insular cortices. *J. Comp. Neurol* 399,440–468. [PubMed: 9741477]
- Shi CJ, Cassell MD, 1998a Cascade projections from somatosensory cortex to the rat basolateral amygdala via the parietal insular cortex. *J. Comp. Neurol* 399,469–491. [PubMed: 9741478]
- Shiple MT, 1982 Insular cortex projection to the nucleus of the solitary tract and brainstem visceromotor regions in the mouse. *Brain Res. Bull* 8, 139–148. [PubMed: 7066705]
- Shura RD, Hurley RA, Taber KH, 2014 Insular cortex: structural and functional neuroanatomy. *J. Neuropsychiatry Clin. Neurosci* 26,276–282. [PubMed: 26037887]
- Soncrant TT, Holloway HW, Rapoport SI, 1986 The pattern of functional coupling of brain regions in the awake rat. *Brain Res.* 369, 1–11. [PubMed: 3697734]
- Stephan KE, 2004 On the role of general system theory for functional neuroimaging. *J. Anat* 205, 443–470. [PubMed: 15610393]

- Uddin LQ, Kinnison J, Pessoa L, Anderson ML, 2014 Beyond the tripartite cognition-emotion-interoception model of the human insular cortex. *J. Cogn. Neurosci* 26,16–27. [PubMed: 23937691]
- Uylings HB, Groenewegen HJ, Kolb B, 2003 Do rats have a prefrontal cortex? *Behav. Brain Res.* 146,3–17.
- Vanegas H, Schaible HG, 2004 Descending control of persistent pain: inhibitory or facilitatory? *Brain Res. Brain Res. Rev* 46,295–309. [PubMed: 15571771]
- Vertes RP, 2006 Interactions among the medial prefrontal cortex, hippocampus and midline thalamus in emotional and cognitive processing in the rat. *Neuroscience* 142,1–20. [PubMed: 16887277]
- Wang Z, Bradesi S, Maarek JM, Lee K, Winchester WJ, Mayer EA, Holschneider DP, 2008 Regional brain activation in conscious, unrestrained rats in response to noxious visceral stimulation. *Pain* 138, 233–243. [PubMed: 18538929]
- Wang Z, Bradesi S, Charles JR, Pang RD, Maarek JM, Mayer EA, Holschneider DP, 2011 Functional brain activation during retrieval of visceral pain-conditioned passive avoidance in the rat. *Pain* 152, 2746–2756. [PubMed: 21944154]
- Wang GQ, Cen C, Li C, Cao S, Wang N, Zhou Z, Liu XM, Xu Y, Tian NX, Zhang Y, Wang J, Wang LP, Wang Y, 2015 Deactivation of excitatory neurons in the prelimbic cortex via Cdk5 promotes pain sensation and anxiety. *Nat. Commun* 6, 7660. [PubMed: 26179626]
- Wang Z, Guo Y, Bradesi S, Labus JS, Maarek JM, Lee K, Winchester WJ, Mayer EA, Holschneider DP, 2009 Sex differences in functional brain activation during noxious visceral stimulation in rats. *Pain* 145, 120–128. [PubMed: 19560270]
- Wang Z, Pang RD, Hernandez M, Ocampo MA, Holschneider DP, 2012 Anxiolytic-like effect of pregabalin on unconditioned fear in the rat: an autoradiographic brain perfusion mapping and functional connectivity study. *Neuroimage* 59, 4168–4188.
- Wang Z, Ocampo MA, Pang RD, Bota M, Bradesi S, Mayer EA, Holschneider DP, 2013 Alterations in prefrontal-limbic functional activation and connectivity in chronic stress-induced visceral hyperalgesia. *PLoS ONE* 8, e59138. [PubMed: 23527114]
- Wehrli HF, Hossain M, Lankes K, Liu CC, Bezrukov I, Martirosian P, Schick F, Reischl G, Pichler BJ, 2013 Simultaneous PET-MRI reveals brain function in activated and resting state on metabolic, hemodynamic and multiple temporal scales. *Nat. Med* 19, 1184–1189. [PubMed: 23975025]
- Wheeler AL, Teixeira CM, Wang AH, Xiong X, Kovacevic N, Lerch JP, McIntosh AR, Parkinson J, Frankland PW, 2013 Identification of a functional connectome for long-term fear memory in mice. *PLoS Comput. Biol* 9, e1002853. [PubMed: 23300432]
- Wiech K, Jbabdi S, Lin CS, Andersson J, Tracey I, 2014 Differential structural and resting state connectivity between insular subdivisions and other pain-related brain regions. *Pain* 155, 2047–2055. [PubMed: 25047781]
- Yasui Y, Breder CD, Saper CB, Ceppetto DF, 1991 Autonomic responses and efferent pathways from the insular cortex in the rat. *J. Comp. Neurol* 303, 355–374. [PubMed: 2007654]
- Zingg B, Hintiryan H, Gou L, Song MY, Bay M, Bienkowski MS, Foster NN, Yamashita S, Bowman I, Toga AW, Dong HW, 2014 Neural networks of the mouse neocortex. *Cell* 156, 1096–1111. [PubMed: 24581503]

HIGHLIGHTS

- Sex differences in insular functional segregation along the anterior-posterior axis.
- Greater insular functional connectivity in female than in male at rest.
- Colorectal distension caused loss of long-range connections and reorganization.
- Sex differences in insular-prefrontal functional connectivity during distension.

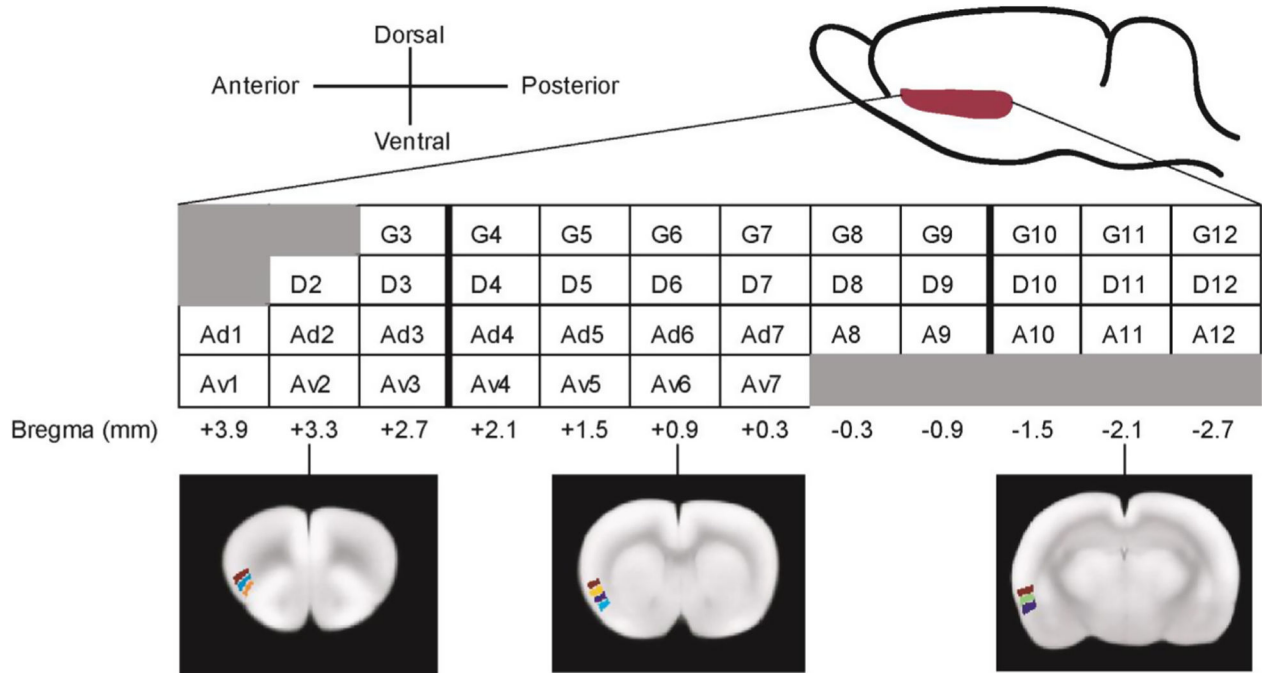
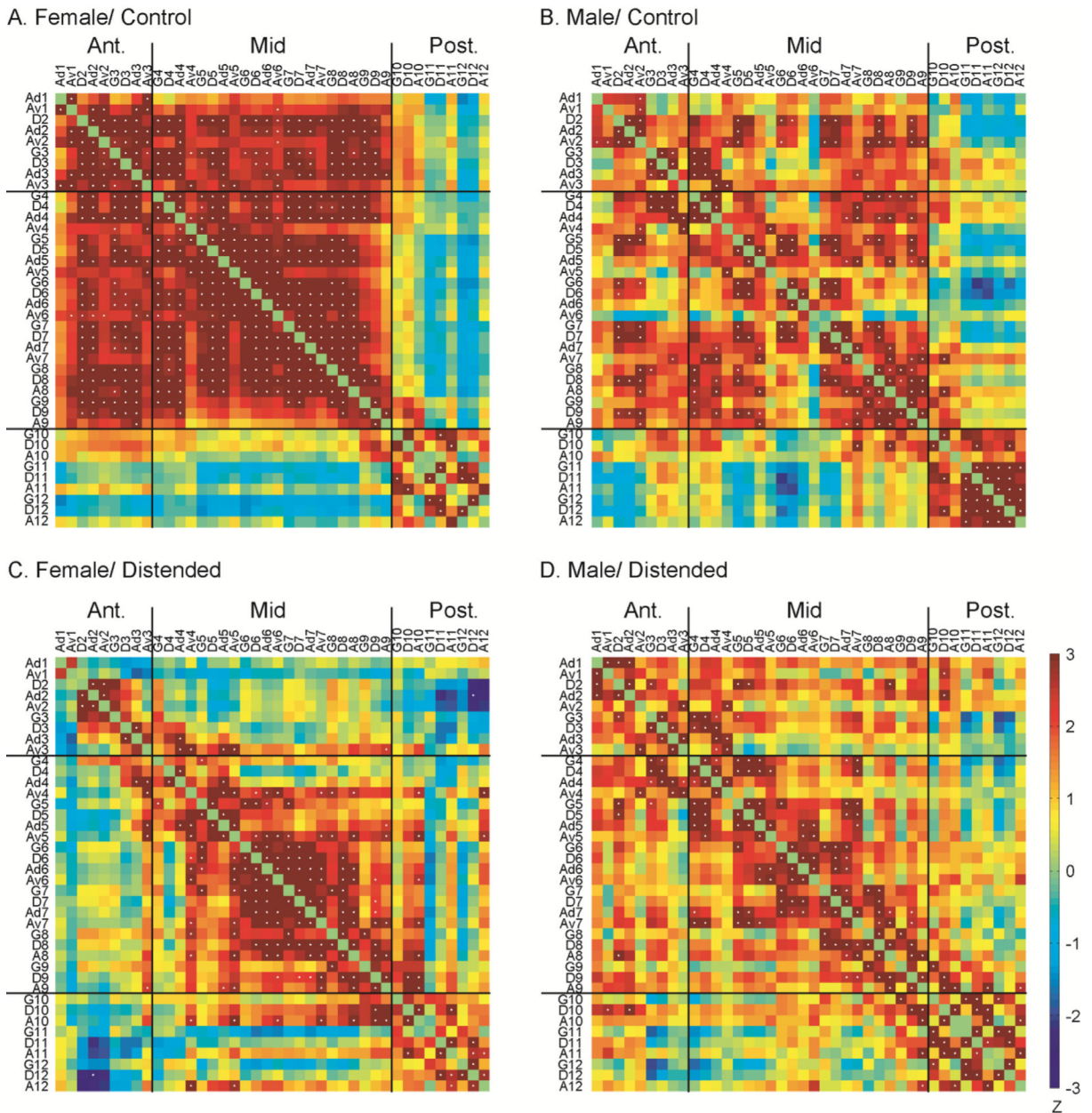
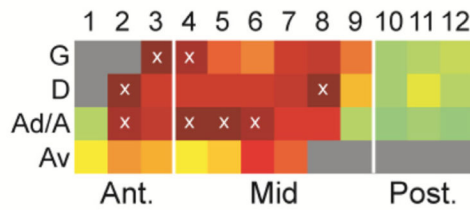


Fig. 1. Region of interest definition for the insular cortex. One ROI is drawn for each cytoarchitectural insular zone on one coronal section of the template brain, with an intersection interval of approximately 0.6 mm. Each ROI label contains an index number denoting its anterior-posterior location. G: granular; D: dysgranular; A: agranular; Ad: dorsal agranular; Av: ventral agranular.

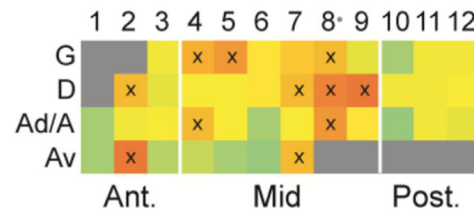
**Fig. 2.**

Intra-insular functional connectivity. Inter-regional correlation matrices show functional connectivity patterns within the insular cortex in the female/control (A), male/control (B), female/distended (C), and male/distended group (D). Z values of Pearson's correlation coefficients are color-coded. Positive and negative correlations are denoted with warm and cold colors, respectively. Statistically significant correlations determined by the jackknife procedure are marked with white dots. Segregations in functional connectivity across the groups suggested a subdivision of the insular into three subregions: an anterior, a mid, and a posterior part. G: granular; D: dysgranular; A: agranular; Ad: dorsal agranular; Av: ventral agranular.

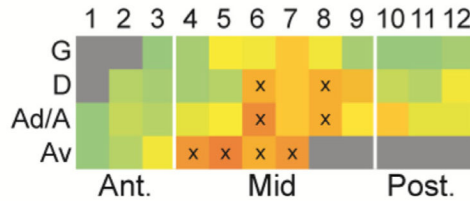
A. Female/ Control



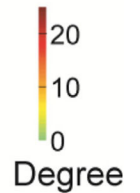
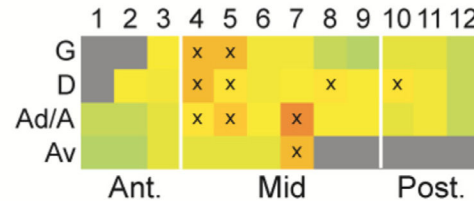
B. Male/ Control



C. Female/ Distended



D. Male/ Distended

**Fig. 3.**

Degree flat map of the intra-insular functional connectivity network. Degree analysis identifies network hubs, which are marked with symbol 'x' in the schematic insular flat map. Sex differences and subregional specificity of intra-insular network hubs are shown. While hubs are located in the anterior and mid INS in the control groups (A, B), they are almost exclusively located in the mid INS in the distended groups (C, D). Also note in female/distended group the emergence of hubs in the Av zone but loss of hubs in the G zone compared to female/control. G: granular; D: dysgranular; A: agranular; Ad: dorsal agranular; Av: ventral agranular.

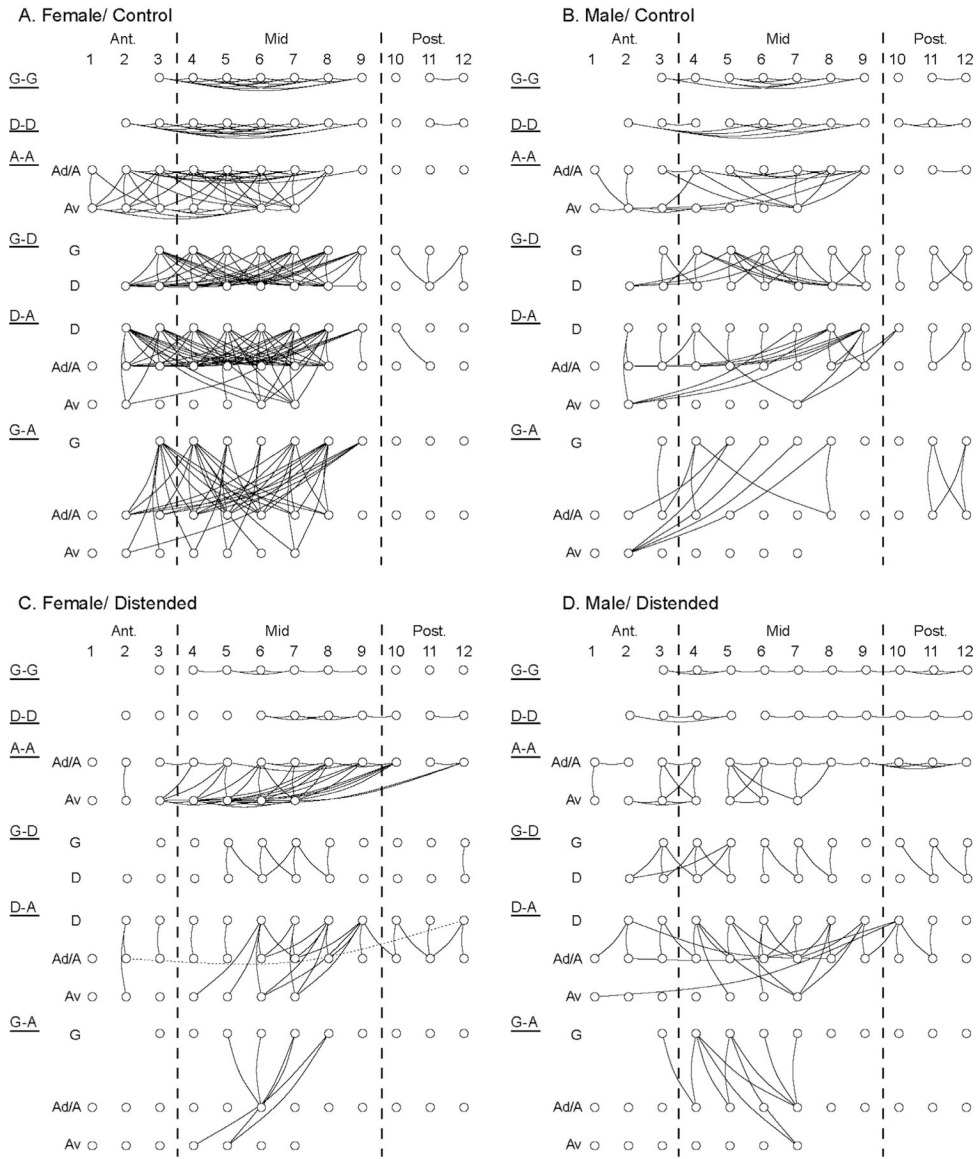
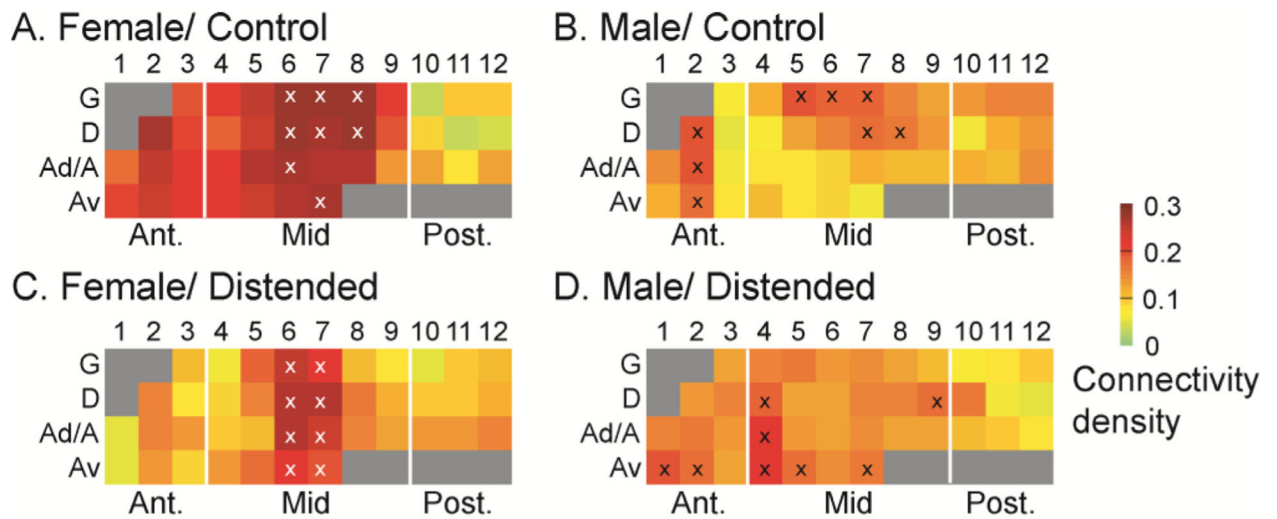


Fig. 4. Sex and CRD-related differences in the pattern of cytoarchitectural zone-specific intra-insular functional connectivity. Within-zone (A-A, agranular; D-D, dysgranular; G-G, granular) and between-zone (D-A, G-D, and G-A) functional connectivity are plotted for the female/control (A), male/control (B), female/distended (C), and male/distended group (D). Ad: dorsal agranular; Av: ventral agranular. This zone-specific visualization of intra-insular network further highlights: loss of long-range connections (long horizontal links) in the distended groups (C, D) compared to the control groups (A, B); loss of G-G and D-D connectivity, as well as anterior-mid INS connectivity in female/distended (C) compared to female/control (A); increased mid-posterior INS connectivity in male/distended (D) compared to male/control (B).

**Fig. 5.**

Whole-brain functional connectivity density of the insular cortex. The female/control group (A) showed the highest level of whole-brain functional connectivity density at 0.20 (mean of 40 ROIs), which was reduced to 0.14 (−30 %) in the female/distended group (C). In contrast, the average connectivity density in the male/control (B) and male/distended group (D) was 0.12 and 0.14 (+17%), respectively. Regions of interest with the highest density (top 20%) are marked with the symbol ‘x’.

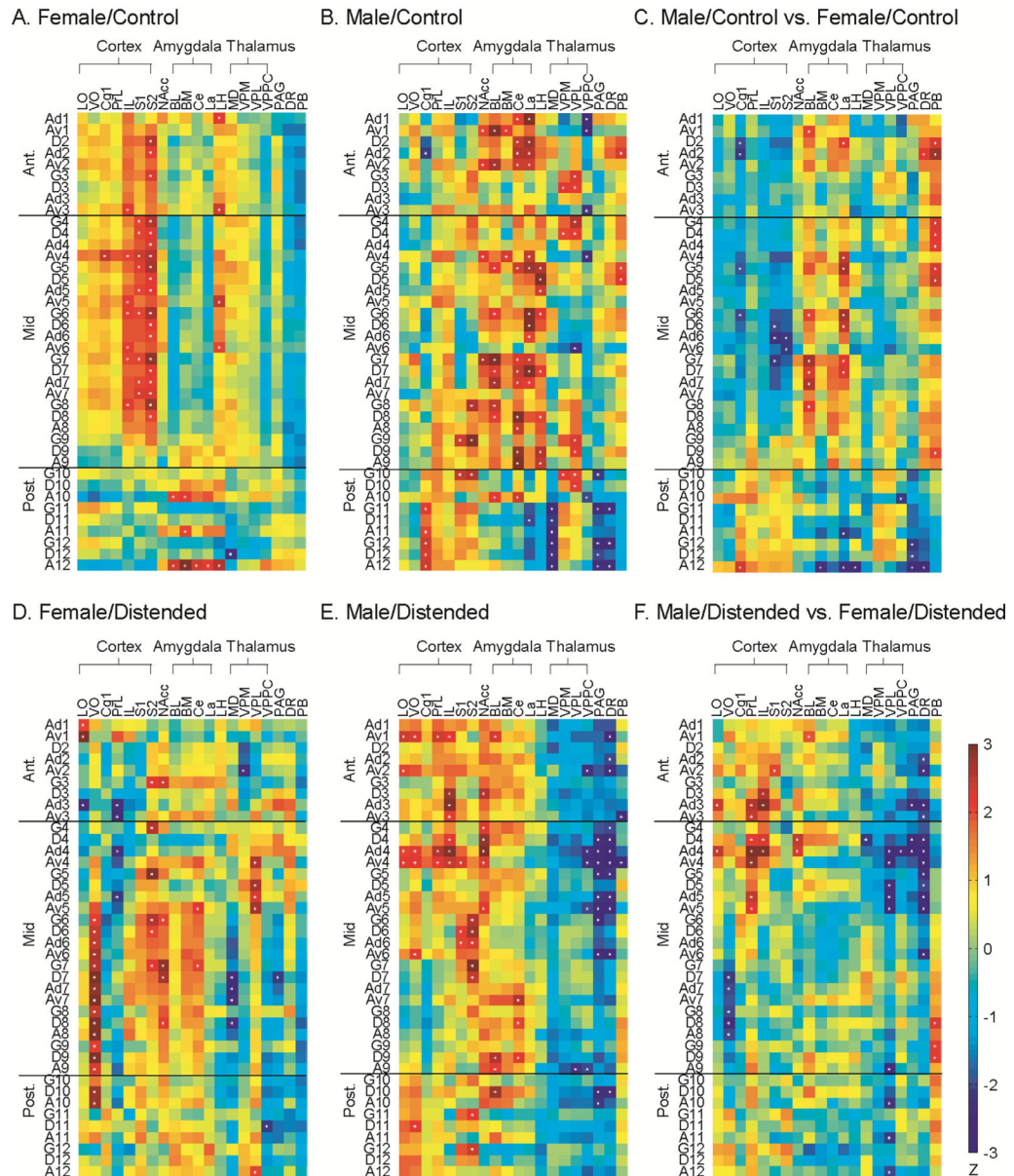


Fig. 6.

Functional connectivity of the insular cortex with pain-related regions. Correlation matrices were calculated for female/control (A), male/control (B), female/distended (D), and male/distended group (E) between the 40 insular regions of interest and 20 brain areas implicated in pain processing with known structural connections with the insular cortex. Significant correlations are marked with white dots. Sex differences in functional connectivity are compared for control (C) and distended groups (F). The matrices of Fisher's Z-statistics represent differences in Pearson's correlation coefficients (r) between males and females. Positive Z values indicate greater r in males, while negative Z values indicate smaller r in males. Significant between-group differences ($P < 0.05$) are marked with white dots. Abbreviations: cortex (LO = lateral orbital, VO = ventral orbital, Cg1 = cingulate area 1, PrL = prelimbic, IL = infralimbic, S1/S2 = primary/secondary somatosensory), NAcc = nucleus

accumbens, amygdala (BL = basolateral, BM = basomedial, Ce = central, La = lateral), LH = lateral hypothalamus, thalamus (MD = mediodorsal, VPM = ventral posteromedial, VPL = ventral posterolateral, VPPC = parvicellular ventral posterior), PAG = periaqueductal gray, DR = dorsal raphe, PB = parabrachial nucleus.

Author Manuscript

Author Manuscript

Author Manuscript

Author Manuscript

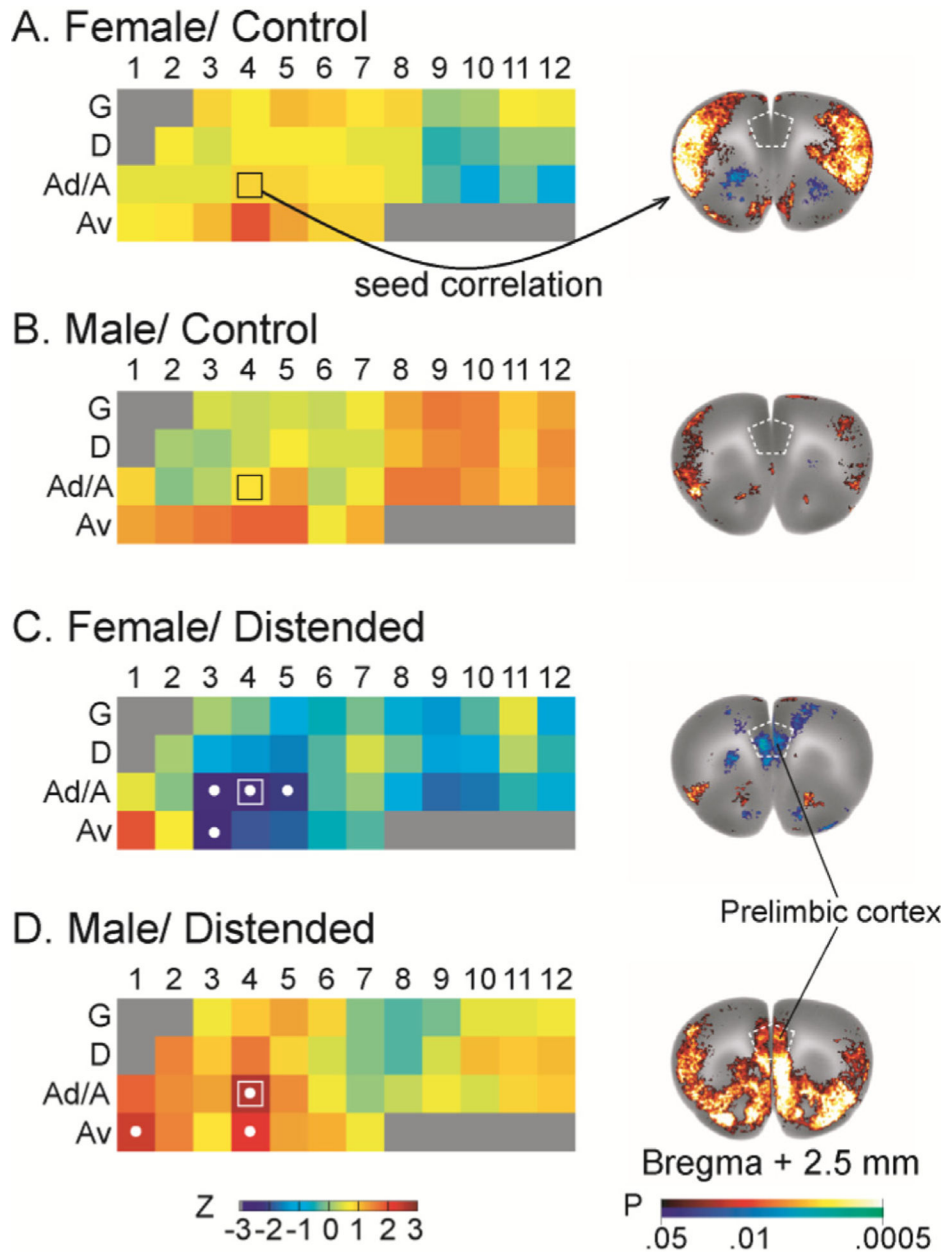


Fig. 7. Sex and CRD-related differences in insular functional connectivity with the prelimbic area of the medial prefrontal cortex. The strength of prelimbic functional connectivity with individual insular region of interest is color coded in insular flat maps (left column, with coding of insular regions as in Fig. 1). Regions showing statistically significant correlations are marked with white dots. Distension induced negative functional connectivity between the anterior/mid insular cortex and the prelimbic cortex in females, but positive connectivity in males. Representative seed correlation results using Ad4 (marked with \square on the flat map) as the seed further showed this striking sex difference (right column). Color-coded overlay over the template brain at bregma +2.5 mm (right column) shows brain areas that are significantly

correlated with the insular seed ($P < 0.05$ for clusters of > 100 contiguous, significant voxels).

Author Manuscript

Author Manuscript

Author Manuscript

Author Manuscript